

An Emulation Platform for Evaluating the Reliability of Deep Neural Networks

*Original*

An Emulation Platform for Evaluating the Reliability of Deep Neural Networks / DE SIO, Corrado; Azimi, Sarah; Sterpone, Luca. - ELETTRONICO. - (2020), pp. 1-4. (Intervento presentato al convegno 33rd IEEE International Symposium on Defect and Fault Tolerance in VLSI and Nanotechnology Systems (DFT 2020) tenutosi a ita nel 19-21 Oct. 2020) [10.1109/DFT50435.2020.9250872].

*Availability:*

This version is available at: 11583/2844426 since: 2020-09-08T10:54:02Z

*Publisher:*

IEEE

*Published*

DOI:10.1109/DFT50435.2020.9250872

*Terms of use:*

This article is made available under terms and conditions as specified in the corresponding bibliographic description in the repository

*Publisher copyright*

IEEE postprint/Author's Accepted Manuscript

©2020 IEEE. Personal use of this material is permitted. Permission from IEEE must be obtained for all other uses, in any current or future media, including reprinting/republishing this material for advertising or promotional purposes, creating new collecting works, for resale or lists, or reuse of any copyrighted component of this work in other works.

(Article begins on next page)

# Long range, high sensitivity, low noise capacitive sensor for tagless indoor human localization

Javed Iqbal, Mihai Teodor Lazarescu, Osama Bin Tariq and Luciano Lavagno  
Department of Electronics and Telecommunications (DET)  
Politecnico di Torino, Italy  
email: {javed\_iqbal; mihai.lazarescu; osama.bintariq; luciano.lavagno}@polito.it

**Abstract**—Capacitive sensors have important advantages and are widely used, but typically up to sensing distances comparable to sensor size. We present the design and experimental results of a self-contained long range capacitive sensor that is suitable for indoor human localization. We make differential measurements of the reactance effects of sensor plate capacitance using a constant excitation frequency, which is both less prone to noise and easier to filter. The experimental results show good sensor sensitivity up to 200 cm for a 16 cm square sensor plate, low noise and good measurement stability.

**Keywords:** Capacitive Sensors; Indoor Human Localization; Health-care Monitoring; Assisted Living; Tagless Human Localization

## I. INTRODUCTION

Indoor human detection, localization, tracking, activity monitoring and identification are very important for many applications, e.g., in health-care monitoring, assisted living and surveillance [1]. J. Rivera-Rubio et. al. present a video-based localization and tracking solution based on simultaneous localization and mapping (SLAM) algorithms [2]. G. Lu et. al. propose a thermal imaging-based indoor localization system, which can localize a person even in dark environments [3]. D. Zhang et. al. present a review of localization techniques for indoor human tracking [4].

Multiple ultrasonic transceivers can be used for indoor human or object localization [5]. Ultrasonic sensing requires a clear line-of-sight to the subject, and the emitted ultrasonic noise can be harmful after long-term exposure [13].

C. Yang and H. R. Shao present a Wi-Fi-based indoor positioning system with multiple Wi-Fi-capable platforms that measure the Time of Arrival (ToA), Angle of Arrival (AoA), Hybrid ToA/AoA and Received Signal Strength (RSS) fingerprinting to localize an object indoors [6]. F. Zahid et. al. discuss various wireless indoor localization techniques, including contactless frequency modulation-based RSS fingerprinting [7]. M. Kok et. al. technique combines ultra-wide band sensors with inertial measurements from a 3-axis accelerometer [8]. Most wireless indoor localization systems are expensive and energy-intensive. Moreover, they suffer from multipath-interference and need a clear line-of-sight [8].

Pyroelectric infrared (PIR) sensors are widely used for indoor human detection, localization and tracking [9], [10], [11]. Recent research also achieves indoor human identification within a small group using PIR sensors [12]. PIR sensors need a restricted field of view for indoor localization applications,

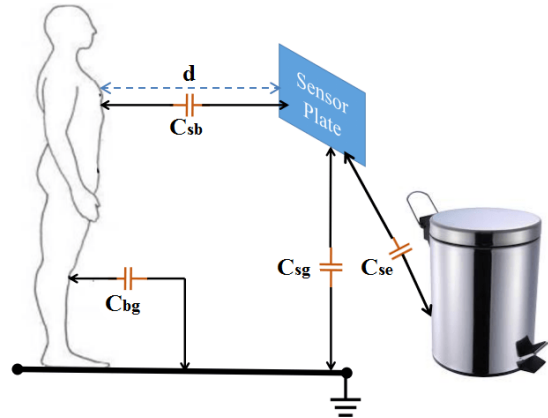


Fig. 1. Capacitance of a load mode capacitive sensor

hence the system requires more sensors which increase the cost. Moreover, the sensors can be triggered by common heat sources, such as sunlight, light bulbs, stoves and heaters.

Human localization based on video and thermal imaging is very accurate, yet rises significant privacy concerns, is expensive, and computation- and energy-intensive.

Other indoor localization techniques can use GPS, RFID, Bluetooth and Smart phone inertial sensors, but they require the person to carry a device or wear a tag [14], [15], [16], [17]. This is not convenient in case of continuous health-care monitoring, and the person may feel uncomfortable or may forget to carry the tag.

Capacitive sensors have been extensively studied due to their low cost, low power consumption and simple realization [1], including their application to indoor human localization, tracking and activity monitoring [18], [19], [20]. Capacitive sensing techniques can also be used for person identification among a small group with distinct physical traits, i.e., different body mass index, weight and physiological structure [21], [22].

The overall capacitance of a load mode or single plate capacitive sensor depends upon the capacitance between the sensor and ground ( $C_{sg}$ ), between the human body and ground ( $C_{bg}$ ), between the sensor and the environment ( $C_{se}$ ) and between the sensor and the human body ( $C_{sd}$ ). The latter depends upon the distance,  $d$ , between the sensor and the human body, as shown in Fig. 1. All capacitances depend also on environmental conditions, like temperature and humidity.

A. R. Akhmareh et. al. present a tagless indoor localization system based on capacitive sensors, tested in a 3 m×3 m room [19]. They make an RC oscillator using the capacitance of the sensor, whose frequency depends thus on the distance to the human body. Since for significant movements far from the sensors (close to the middle of the room) the capacitance variations can be much less than 0.01%, the authors applied several noise reduction techniques. For instance, to reduce the quantization noise they measure the oscillation frequency by counting the periods for one second, and to reduce the environmental noise they average 20 measurements for each position in the room. Hence, the acquisition time for one location is 20 seconds, which makes the system unpractical for most real time uses. Moreover, the 555-based RC oscillator that they used is very sensitive to voltage noise, hence to most environmental noise captured by the capacitive sensor plate. This noise can be filtered only in the base band, which significantly reduces filter efficiency and, combined with other factors, lead to very poor sensor sensitivity beyond 100 cm.

The performance of an indoor localization system strongly depends on the performance of the sensors. In this work, we present the design and experimental results obtained with a novel sensor front-end interface design circuitry that improves the sensor sensitivity, range, response time and noise rejection.

The rest of the article is organized as follows. In Section II we discuss our main contributions. Section III explains our methodology, i.e., the capacitive sensor front-end interface circuit design and the experimental setup. In Section IV we present the experimental results and in Section V we critically discuss them. In Section VI we consider some directions for future work and improvements. Section VII provides some conclusions drawn from our work.

## II. OUR MAIN CONTRIBUTIONS

A recent survey on capacitive sensing provides comprehensive details of ongoing research on indoor localization using capacitive sensors and the challenges involved [1]. It reports only 12 works that discuss sensing ranges from 100–300 cm, while most research focuses on much shorter ranges. Some of the major research challenges involve sensitivity, noise and sensing range.

In this work, we present the design, implementation and experimental results of a capacitive sensor node. With a plate of 16 cm×16 cm we obtained sufficient sensitivity up to a 200 cm range, a high resolution and low noise. We hold that with one sensor on each wall of a square 4 m×4 m room we can accurately localize a person within the room, hence significantly increasing the sensing range and localization reliability with respect to past work [19].

## III. METHODOLOGY

### A. Capacitive-Sensor Front-end Interface Design

The front-end interface circuitry of the sensor is shown in Fig. 2. It is designed to measure the difference in phase and amplitude introduced on the same  $V_{in}$  sine wave excitation by

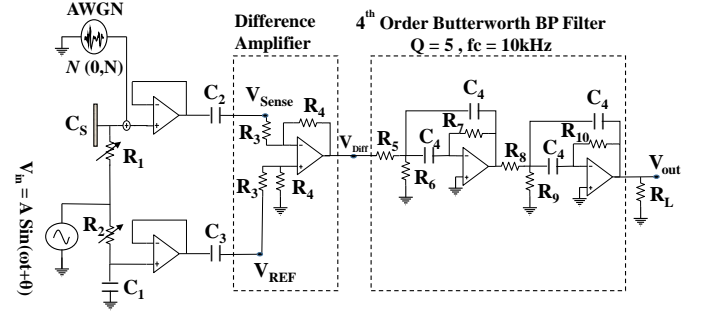


Fig. 2. Capacitive sensor front-end interface circuit design

two RC low-pass filters:  $R_1 C_S$  which is variable with  $C_S$  (the total capacitance of the sensor plate) and a fixed one,  $R_2 C_1$ .

The filter outputs are read using two identical high-impedance voltage repeaters. Capacitors  $C_2$  and  $C_3$  eliminate DC offsets from the repeater outputs before they enter a difference amplifier.  $R_2$  and  $C_1$  are fixed, hence  $V_{Ref}$  has a constant magnitude and phase, whereas the changes in the value of  $C_S$  change the magnitude and phase of  $V_{Sense}$ . The difference amplifier subtracts  $V_{Sense}$  from  $V_{Ref}$  and amplifies the difference signal by  $G = \frac{R_4}{R_3}$ . The amplitude of the difference signal,  $V_{Diff}$ , is modulated by the changes in the value of  $C_S$ , the total capacitance of the sensor plate. The noise on the modulated carrier  $V_{Diff}$  is removed using two narrow band high Q-factor band-pass filters.

The mathematical model of the front-end interface circuitry is as follows:

$$V_{in} = A \sin(\omega t + \theta) \quad (1)$$

where  $\omega = 2\pi f$ . In our experiments we set  $f = 10$  kHz.

We are only interested in the steady state response, so we can assume that  $\theta = 0$ . Rewriting in phasor form we obtain:

$$V_{in} = A \angle 0^\circ \quad (2)$$

$$V_{Ref} = A_2 \angle \phi_2 = A_2 e^{j\phi_2} = A_2 (\cos\phi_2 + j\sin\phi_2) \quad (3)$$

We model the environmental noise that enters the circuit through the sensor plate as a zero-mean additive white Gaussian (AWGN), as shown in Fig. 2 and Fig. 4. Thus we have:

$$V_{Sense} = A_1 \angle \phi_1 + N(0, N) = A_1 e^{j\phi_1} + N(0, N) \quad (4)$$

$$V_{Sense} = A_1 (\cos\phi_1 + j\sin\phi_1) + N(0, N) \quad (5)$$

$$\begin{aligned} V_{Diff} &= \frac{R_4}{R_3} [V_{Ref} - V_{Sense}] + N(0, N) \quad (6) \\ &= \frac{R_4}{R_3} [(A_2 \cos\phi_2 - A_1 \cos\phi_1) - j(A_2 \sin\phi_2 + A_1 \sin\phi_1)] \\ &\quad + N(0, N) \quad (7) \end{aligned}$$

We remove the additive noise using a narrow band, 4th-order Butterworth bandpass filter centered on the excitation frequency (10 kHz) with a quality factor  $Q = 5$ , as shown in Fig. 2. The measured response of the filter is shown in Fig. 3. At the output of the filter we have:

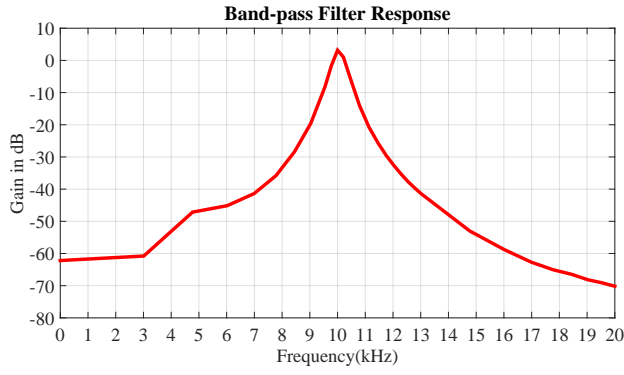


Fig. 3. Measured response of the 4th-order Butterworth bandpass filter with  $f_c = 10$  kHz and  $Q = 5$ .

$$V_{out} = \frac{R_4}{R_3} (A_2 \cos \phi_2 - A_1 \cos \phi_1) - j \frac{R_4}{R_3} (A_2 \sin \phi_2 + A_1 \sin \phi_1) \quad (8)$$

with

$$|V_{out}| = G \sqrt{A_1^2 + A_2^2 + 2A_1 A_2 \cos(\phi_2 - \phi_1)} \quad (9)$$

where:

$$G = \sqrt{\frac{R_4}{R_3}} \quad (10)$$

$$A_1 = \frac{1}{\sqrt{1 + (\omega C_S R_1)^2}} \quad (11)$$

$$A_2 = \frac{1}{\sqrt{1 + (\omega C_1 R_2)^2}} \quad (12)$$

$$\phi_1 = -\arctan(\omega C_S R_1) \quad (13)$$

$$\phi_2 = -\arctan(\omega C_1 R_2) \quad (14)$$

(9)-(14) provide a closed form analytical model of our capacitance-to-voltage converter, shown in Fig. 2. All the parameters are fixed in (10)-(14) except for  $C_S$ , hence

$$|V_{out}| = f(C_S). \quad (15)$$

As argued in Section I,  $C_S$  depends on many variables, some of which are long-term constants (like furniture settings in the room), some are long-term stationary random processes (like the relative humidity and temperature), and some are non-stationary random processes (like swift movement of the human body, movement of electronic devices and metallic objects etc. Hence, we have

$$C_S = f(d, C_{sg}, C_{bg}, C_{se}, RH, T, \dots), \quad (16)$$

where RH is the relative humidity and T is the temperature.

As shown by (15) and (16), we need to treat the voltage output of the sensor vs. distance  $d$  of the human body from the sensor as a stochastic process.

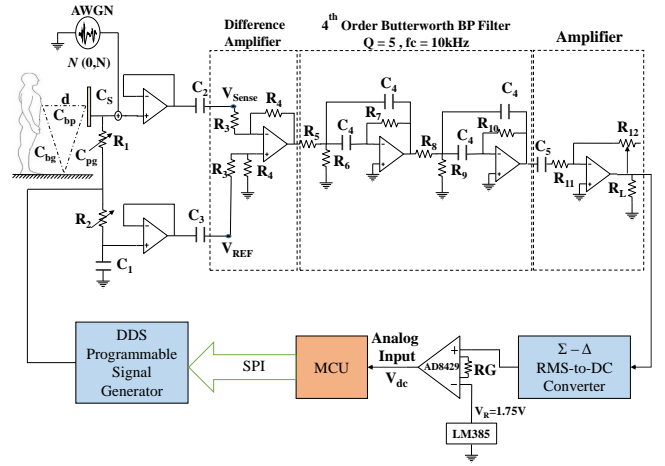


Fig. 4. Experimental Setup

### B. Experimental Setup

Fig. 4 shows the experimental setup we have used to characterize the voltage response of the sensor to the distance  $d$  of the human body from the sensor. The front-end interface circuitry has been presented in Section III-A. We used an AD9837 DDS Programmable signal generator programmed through the SPI interface of an ATmega328P microcontroller to generate the 10 kHz sine wave excitation. The filtered output,  $V_{out}$ , is further amplified before being demodulated using a precision  $\Sigma$ - $\Delta$  RMS-to-DC converter, which converts the amplitude of the signal to a DC level.

For best sensitivity, we should tune the cutoff frequency of both RC filters to match the 10 kHz excitation frequency, while there is nobody near the sensor (by adjusting  $R_1$  and  $R_2$ ), hence

$$A_1 = A_2 = \frac{1}{\sqrt{2}}$$

and

$$\phi_1 = \phi_2 = -\frac{\pi}{4}$$

In this case, according to (9) we get  $V_{out} = 0$ . But any  $C_S$  variations around this value would cause always a zero or positive output, hence a non-monotonic dependency of the sensor output on  $C_S$  variations, which would make the sensor unusable for localization.

To ensure that the sensor response is always monotonic, we need to never have the two RC branches balanced, for any possible  $C_S$  value. For this, we exploit the fact that  $C_S$  is lower bound, which is its value when no person is in sensor range. For that minimum  $C_S$ , we tune  $R_1$  to match the cutoff frequency of the  $R_1 C_S$  filter to the excitation frequency, 10 kHz. Then we detune the  $R_2 C_1$  filter from the excitation frequency such way that for all  $C_S$  values, the  $R_1 C_S$  filter will never match the  $R_2 C_1$  one. In fact,  $V_{Ref}$  will always lead  $V_{Sense}$  in phase for any body-sensor distance  $d$ .

While this technique ensures a monotonic response of the sensor, it also introduces a minimum non-zero output which

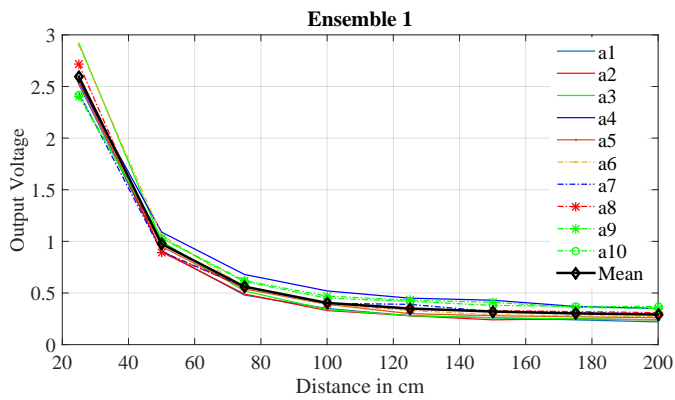


Fig. 5. Measurements taken on day 1 (a sunny day)

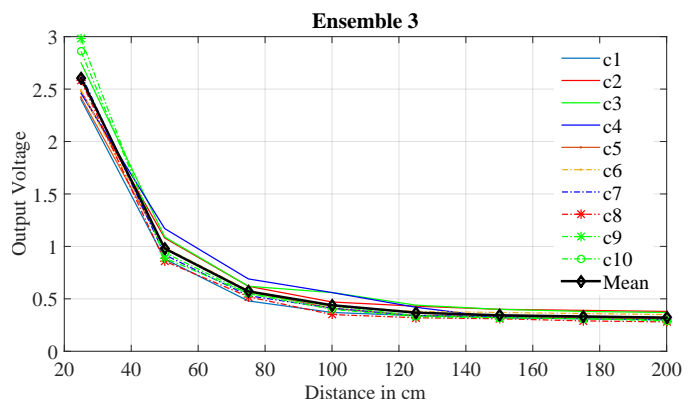


Fig. 7. Measurements taken on day 2 (little rain)

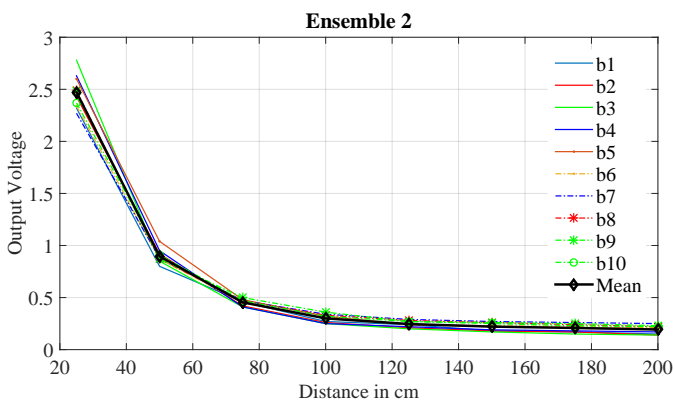


Fig. 6. Measurements taken on day 1 (a sunny day)

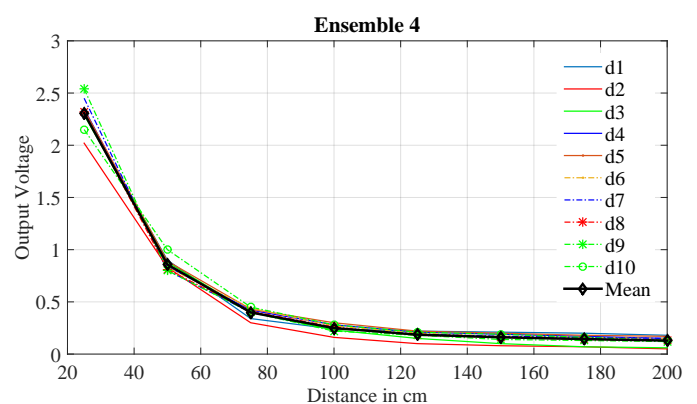


Fig. 8. Measurements taken on day 3 (heavy rain)

corresponds to the minimum  $V_{Ref}$  lead in phase. This output limits the amplification of the slight modulations due to the movement of the person, because it can lead quickly to saturation of the amplifier output. Hence, to be able to amplify to reach a good sensitivity, we subtract a constant voltage from the output and amplify the difference signal, as shown in Fig. 4. The DC output of the instrumentation amplifier is then sampled and recorded by the microcontroller (MCU).

#### IV. EXPERIMENTAL RESULTS

Due to the stochastic nature of measurements, we took multiple measurements at different times over three days, for different environmental conditions (i.e., environmental humidity and temperature). Each set of measurements contains 10 samples of measurements taken at distances body-sensor from 25 cm to 200 cm, in 25 cm increments. Fig. 5 to Fig. 9 show measurement sets along with their means. Fig. 5 and Fig. 6 show measurements taken on a sunny day. Fig. 7 shows measurements taken on a day with drizzle, while Fig. 8 and Fig. 9 show measurements taken on a heavy rain day. Fig. 10 shows the averages of all measurement sets.

The experimental results show the very good sensitivity of the sensor. Even a position change far away from sensor, from 200 cm to 175 cm, yields a consistent 11 mV output change. Table I

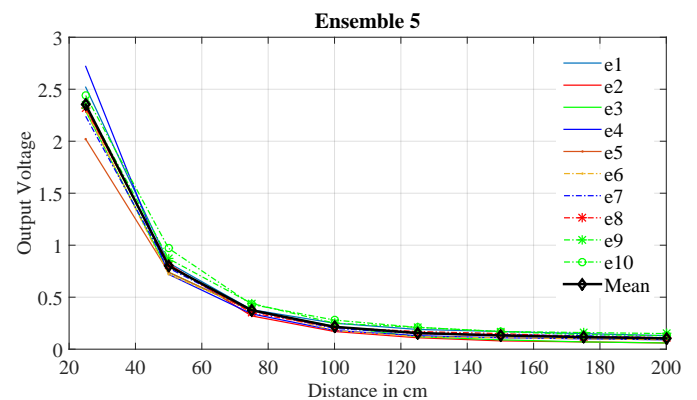


Fig. 9. Measurements taken on day 3 (heavy rain)

TABLE I  
AVERAGE  $V_{dc}$  VS. BODY-SENSOR DISTANCE AND OUTPUT VOLTAGE INCREMENTS FOR 25 CM STEP TOWARDS THE SENSOR

Distance (cm)	Average $V_{dc}$ (V)	Output change (mV)
200	0.2910	—
175	0.3020	11
150	0.3200	18
125	0.3500	30
100	0.4040	54
75	0.5620	158
50	0.9760	414
25	2.5960	1620

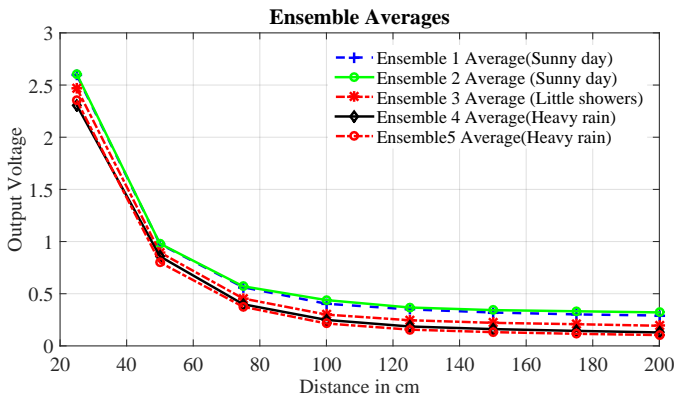


Fig. 10. Ensemble averages

shows the output voltage of the sensor vs. distance from the sensor, along with the output changes for each 25 cm step towards the sensor.

Fig. 10 shows that under static room settings and the same environmental conditions, the system behaviour is almost stationary. However, these conditions cannot be expected to remain constant over long periods.

## V. DISCUSSION

### A. Trend stability

The mean curves in Fig. 10 show a similar trend, but with a time random offset. We can write

$$V_{dc} = f(d) + e_t, \quad (17)$$

where  $f(d)$  is the functional dependency on body distance and  $e_t$  is a stationary random mean shift. The mean shift is a common problem, which is often encountered in stochastic systems. The solution to this problem will be discussed in Section V-C.

### B. Advantages of the proposed sensor

The proposed sensor is composed of inexpensive hardware with low power consumption. With some consumption optimization, it is possible to implement a self-contained long lifetime battery powered sensor node.

Our sensor features fast responsiveness. It can provide continuous readings and has very small transients. This provides opportunity to reduce the energy consumption through duty cycled operation, as discussed in Section VI-B.

Furthermore, the amplitude modulated carrier frequency allows to remove most noise using narrow bandpass filters.

### C. Observed shortcomings and proposed solutions

Fig. 10 shows the problem of random mean shift which, according to our observation, mostly depends on the changing environmental conditions like temperature, humidity or more precisely relative humidity (RH). This problem could be resolved using derivatives of the measured data instead of the absolute values, hence removing the momentarily constant offset from the measured data. Another hardware-based solution

may be to install temperature and humidity sensors on the sensor node, and use their readings to compensate the output offset of the capacitive sensor.

We built our prototype using easily available components. The micropower adjustable voltage reference, LM385 has an error of 1-2%, which may cause serious errors in the output. This issue can be resolved by using a precise voltage reference.

## VI. FUTURE WORK

### A. Multiple Sensor nodes in WSN Configuration

To accurately localize a person in a room, we intend to use multiple sensor nodes in a wireless sensor network (WSN) configuration, in order to acquire a large data set which contains measurements of multiple sensors for each location of the person in the room. Later, we will use this data for training and classification purpose, as in [19].

### B. Hardware Optimization and Power Management

As most of the time the persons remain stationary or move slowly indoor, the sensor can be operated with variable duty cycle adapted to person activity to further reduce the energy consumption. Moreover, we can use low voltage and low-power components to reduce the power consumption of the sensor node.

## VII. CONCLUSION

From our experimental results, we conclude that our developed sensor shows a very good sensitivity as shown in Table I. It has a long sensing range (200 cm), which makes it possible to use multiple sensors to localize a person in a 4 m×4 m room. The sensor output has a very low noise level compared with the past work, which makes it easy to handle during pre- and post-processing of data. Our sensor has a simple and low cost front-end interface design and provides a low noise and low power solution for indoor human localization.

## ACKNOWLEDGMENT

The authors would like to thank Arslan Arif and Zohaib Aziz Mehtar, who helped us during the execution of our experiments.

## REFERENCES

- [1] T. Grosse-Puppenthal et. al., "Finding Common Ground: A Survey of Capacitive Sensing in Human-Computer Interaction", ACM CHI Conference on Human Factors in Computing Systems, May 06–11, 2017.
- [2] J. Rivera-Rubio, I. Alexiou, and A.B. Anil, "Appearance-based indoor localization: A comparison of patch descriptor performance", Pattern Recognition Letters, volume 66, pp. 109–117, 2015.
- [3] G. Lu et. al., "Where am i in the dark: Exploring active transfer learning on the use of indoor localization based on thermal imaging", Neurocomputing, volume 173, pp. 83–92, 2016.
- [4] D. Zhang et. al., "Localization technologies for indoor human tracking", 5th International Conference on Future Information Technology (FutureTech), pages 1–6, 2010.
- [5] L. Mainetti, L. Patrono and I. Sergi, "A survey on indoor positioning systems", 22nd International Conference on Software, Telecommunications and Computer Networks (SoftCOM), pp. 111–120, 2014.
- [6] Yang, Chouchang and Shao, Huai-Rong, "WiFi-based indoor positioning", IEEE Communications Magazine, volume 53, number 3, pp. 150–157, 2015.

- [7] F. Zahid et. al., "Recent advances in wireless indoor localization techniques and system", *Journal of Computer Networks and Communications*, volume 2013, 2013.
- [8] M. Kok et. al., "Indoor positioning using ultrawideband and inertial measurements", *IEEE Transactions on Vehicular Technology*, volume 64, number 4, pp. 1293–1303, 2015.
- [9] J. Yun and MH. Song, "Detecting direction of movement using pyroelectric infrared sensors", *IEEE Sensors Journal*, volume 14, number 5, pp. 1482–1489, 2014.
- [10] D. Yang et. al., "Indoor human localization using PIR sensors and accessibility map", *IEEE International Conference on Cyber Technology in Automation, Control, and Intelligent Systems (CYBER)*, pages 577–581, 2015.
- [11] S. Narayana et. al., "PIR sensors: Characterization and novel localization technique", *Proceedings of the 14th International Conference on Information Processing in Sensor Networks*, pp. 142–153, 2015.
- [12] J. Yun and SS. Lee, "Human movement detection and identification using pyroelectric infrared sensors", *Sensors*, volume 14, number 5, pp. 8057–8081, 2014.
- [13] B Smagowska et. al., "Effects of ultrasonic noise on the human bodya bibliographic review", *International Journal of Occupational Safety and Ergonomics*, volume 19, number 2, pp. 195–202, 2013.
- [14] N. Fallah et. al., "Indoor human navigation systems: A survey", *Interacting with Computers*, 2013.
- [15] A. Athalye et al., "Novel semi-passive RFID system for indoor localization", *IEEE Sensors Journal*, volume 13, number 2, pp. 528–537, 2013.
- [16] Y. Zhuang et al., "Smartphone-based indoor localization with bluetooth low energy beacons", *Sensors*, volume 16, number 5, pages 596, 2016.
- [17] Z. Yang et. al., "Mobility increases localizability: A survey on wireless indoor localization using inertial sensors", *ACM Computing Surveys (CSUR)*, volume 47, number 3, pp. 54, 2015.
- [18] Arshad et. al., "An activity monitoring system for senior citizens living independently using capacitive sensing technique", *Instrumentation and Measurement Technology Conference Proceedings (I2MTC), 2016 IEEE International*, pp. 1–6, 2016.
- [19] A. R. Akhmareh, M. T. Lazarescu, O. B. Tariq and L. Lavagno, "A Tagless Indoor Localization System Based on Capacitive Sensing Technology", *Sensors*, volume 16, number 9, pp. 1448, 2016.
- [20] A. Braun, R. Wichert, A. Kuijper, and D. W. Fellner, "Capacitive proximity sensing in smart environments", *Journal of Ambient Intelligence and Smart Environments*, volume 7, number 4, pp. 483–510, 2015.
- [21] D. Wang, "Basics of Capacitive sensing and Application", *Texas instruments*, December, 2014.
- [22] J. Iqbal, A. Arif, O.B. Tariq, M.T. Lazarescu and L. Lavagno, "A contactless sensor for human body identification using RF absorption signatures", *IEEE Sensors Applications Symposium (SAS2017), Glassboro, New Jersey, USA*, 2017.